PNAS
www.pnas.org

Supplementary Information for

Low-Energy Electron Holography Imaging of Conformational Variability of Single Antibody Molecules from Electrospray Ion Beam Deposition

Hannah Ochner[a], Sven Szilagyi[a], Sabine Abb[a], Joseph Gault[b], Carol V. Robinson[b], Luigi Malavolti[a], Stephan Rauschenbach[a,b], and Klaus Kern[a,c]

[a]Max Planck Institute for Solid State Research, Heisenbergstr. 1, DE-70569 Stuttgart, Germany
[b]Department of Chemistry, University of Oxford, 12 Mansfield Road, Oxford OX1 3TA, UK
[c]Institut de Physique, École Polytechnique Fédérale de Lausanne, 1015 Lausanne, Switzerland

Corresponding author : Luigi Malavolti
Email: l.malavolti@fkf.mpg.de

This PDF file includes:

Supplementary Information Text

Model of antibody flexibility. The model presented in the main text generates new structures starting from the PDB model 1IGT by considering all the possible permutations of the φ and ψ angles of the Gly 236 residues of both heavy chains, see Fig. S2, for rotation angles of 0°, 60°, 120°, 180°, 240°, 300°. The 0° rotation refers to the angle observed in the original PDB model. This procedure generates $6^4 = 1296$ different configurations. The subset of roughly 400 structures that show no relevant steric hindrance, i.e. no overlap of the subunit backbones, was considered for the data interpretation.
The φ and ψ angles of the Gly 236 residues were selected for this analysis since these residues are part of the hinge region connecting the Fc subunit with the two Fab subunits. Additionally, the hinge region is stabilized by disulfide bonds interconnecting the two heavy chains. The modification of the φ and ψ angles of both Gly 236 residues avoids the alteration of these disulfide bonds.

Denatured antibodies. Creating experimental conditions that do not support native protein conformations leads to a clear difference both on the level of the mass spectrum and regarding the structures observed on the surface. To achieve such conditions, we prepared a solution with 15µl AB stock (1mg/ml) + 185µl AmAc (200mM) + 100µl EtOH + 1µl formic acid to denature the proteins in solution. Additionally, we increased the temperature at the interface to 130°C and applied an ionization voltage of 2660V.
The mass spectrum of denatured antibodies differs significantly from that of folded antibodies (see Fig. S5a). Instead of narrow peaks that can be assigned to specific charge states of the folded protein, the denatured mass spectrum features a broad intensity distribution over a wide range of masses in a lower m/z range than the range in which the peaks corresponding to folded proteins appear. The lack of resolved peaks in the denatured spectrum is due to the limited resolution of our linear time-of-flight instrument. The change in conformation is also reflected in the size distribution of the molecules found on the surface. In comparison to the size distribution observed for molecules in collapsed conformation deposited from native solution conditions (Fig. 5a-b), the length distribution of the denatured molecules is broadened, and the width distribution is shifted to significantly smaller values (see Fig. S5b-c).

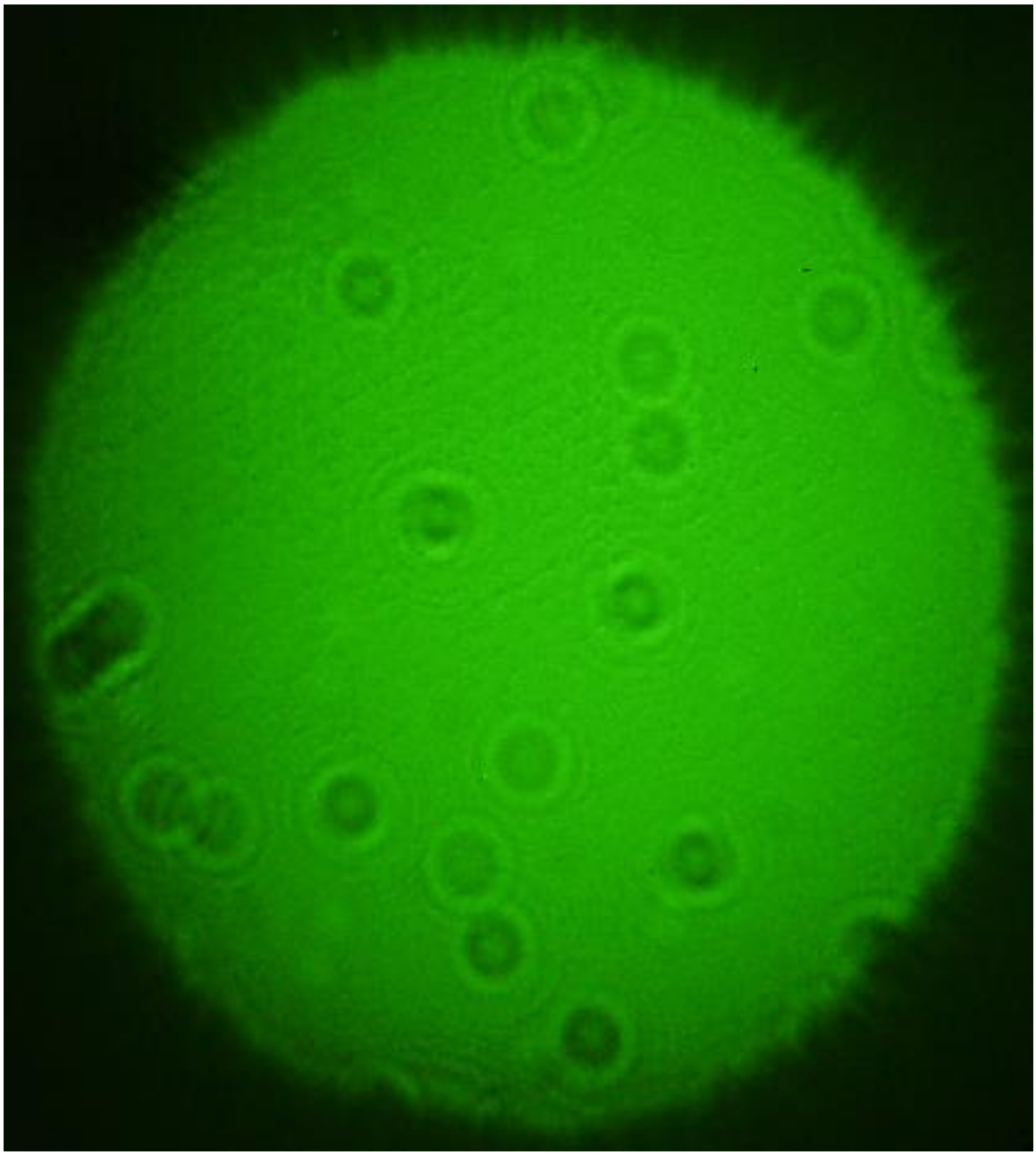

Fig. S1. Survey image of one of the graphene-covered holes of the TEM grid, the diameter of the hole is 500 nm. While there are several molecules deposited on that hole, the coverage is such that they are far apart from one another, which yields isolated protein molecules.

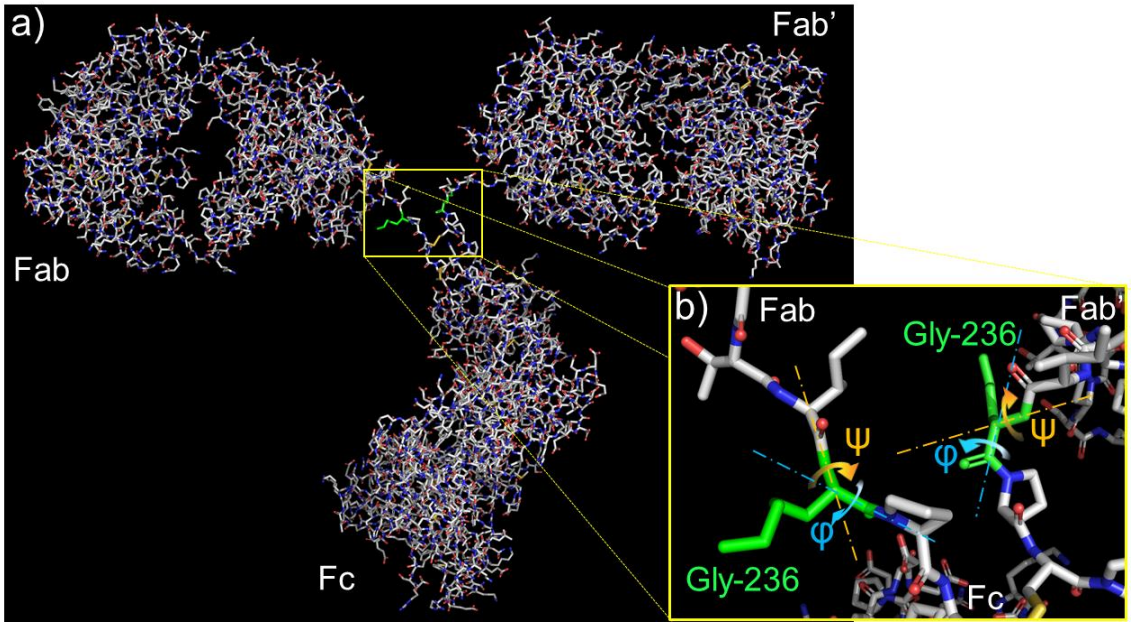

Fig. S2. a) Ball and stick representation of the 1IGT X-ray crystallographic structure with the two Gly-236 residues highlighted in green. b) A close-up view of the hinge region around the two Gly-236 residues (yellow rectangle in a)). The pale blue and orange arrows represent the rotations corresponding to a change of the φ and ψ angles, respectively; the rotation axes are depicted as dashed lines. The color scheme used in both panels is: carbon in light gray, oxygen in red, nitrogen in blue and sulfur in yellow.

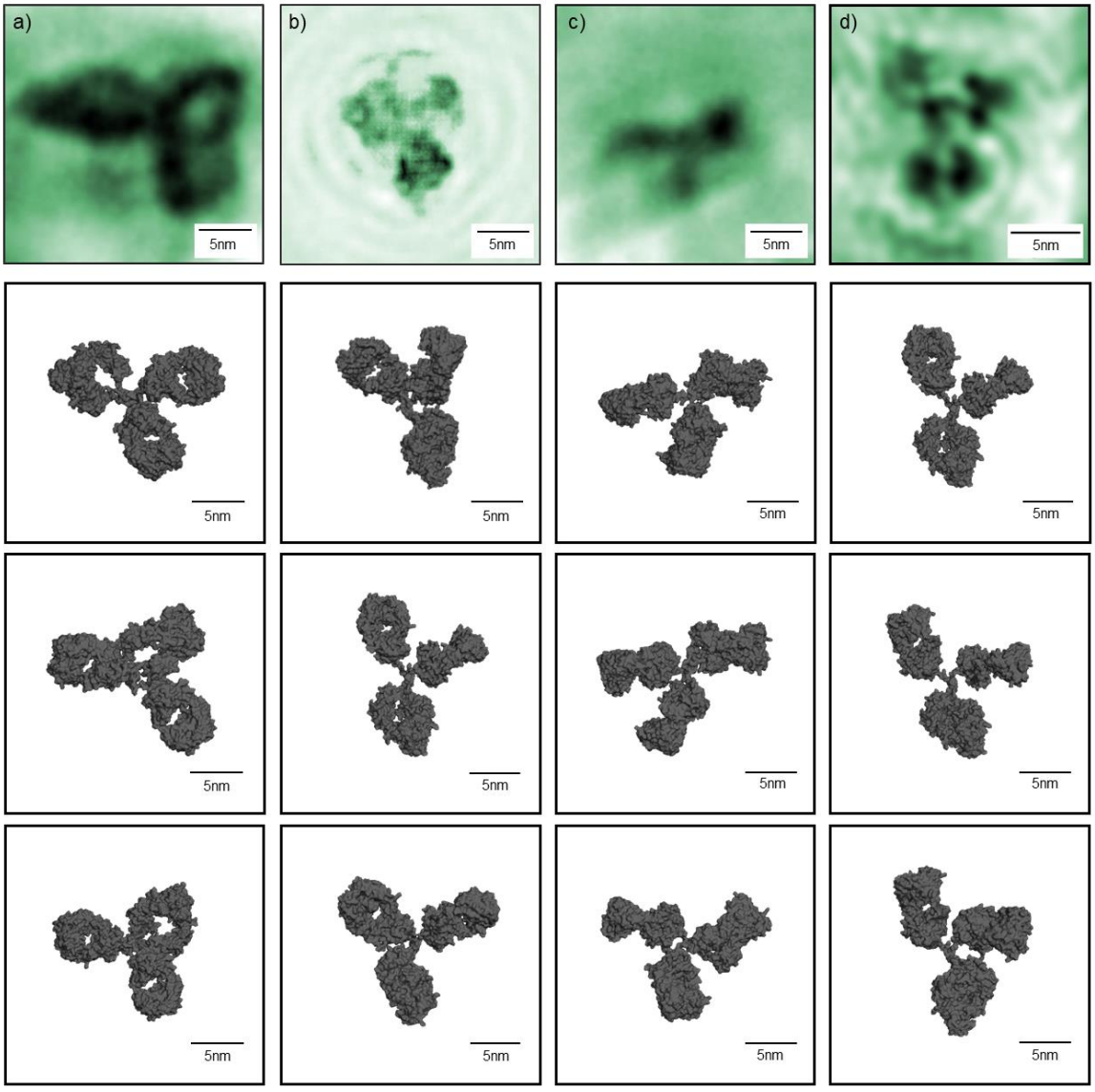

Fig. S3. Comparison of experimental data with several conformations obtained from the model described in Fig. S2. For each experimentally obtained image, several model conformations can be found that fit the experimental conformation in both size and shape.

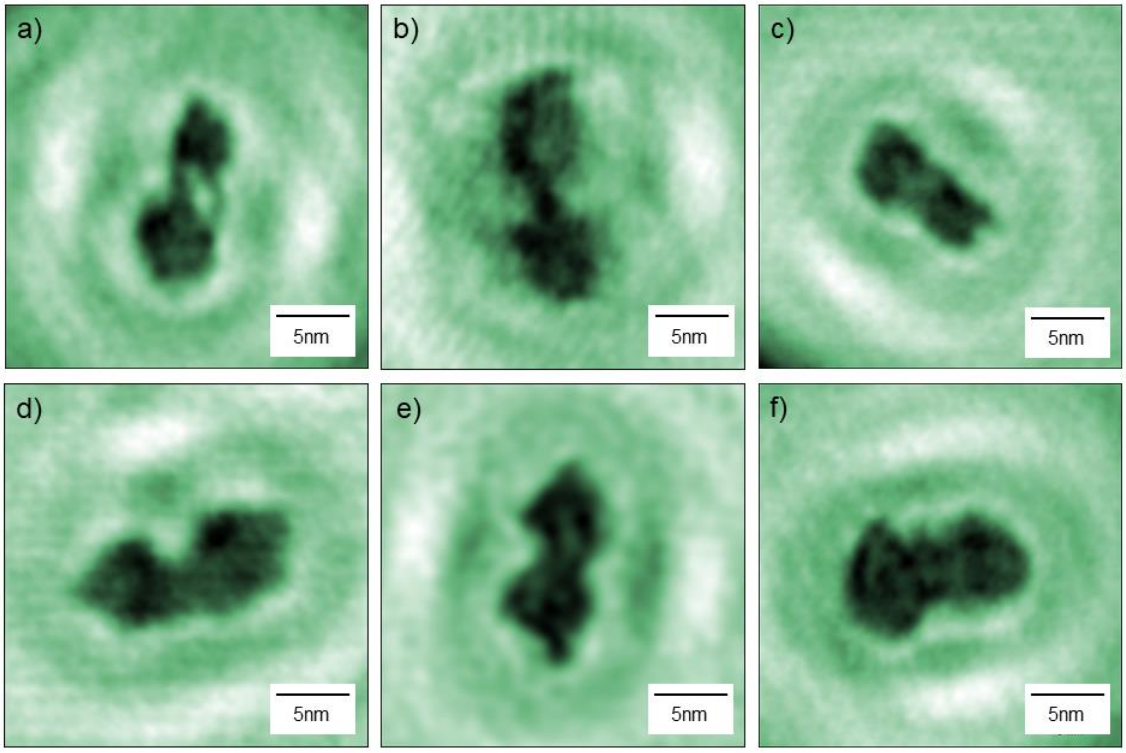

Fig. S4. The experimental data yields a range of conformations that can be classified as vertical geometries with two distinguishable subunits. As shown in this figure, this includes conformations with a clearly discernible hinge region (a, b), regions of lower contrast between the subunits (c), touching subunits (d, e) and subunits blending into each other (f).

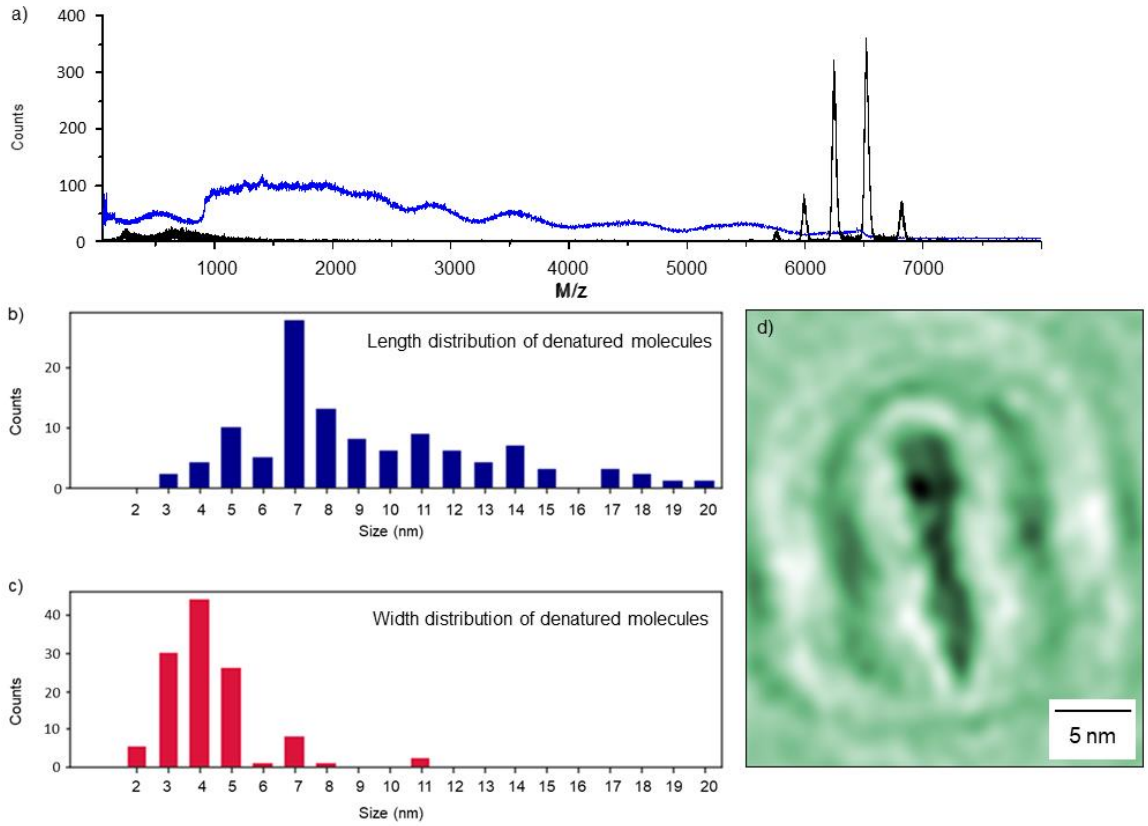

Fig. S5: a) Mass spectra of denatured antibodies (blue) and native antibodies (black). The lack of resolved peaks in the denatured spectrum is due to the limited resolution of our mass spectrometer. b) Length distribution of denatured antibodies measured by LEEH. c) Width distribution of denatured antibodies measured by LEEH. d) Reconstruction of a denatured antibody molecule measured by LEEH.